

THE TAXONOMIC STATUS OF THE PLIOCENE CAPYBARAS (RODENTIA) *PHUGATHERIUM* AMEGHINO AND *CHAPALMATHERIUM* AMEGHINO



MARÍA G. VUCETICH¹, CECILIA M. DESCHAMPS², MARÍA E. PÉREZ³ AND CLAUDIA I. MONTALVO⁴

¹División Paleontología Vertebrados, Museo de La Plata, Paseo del Bosque s/ n, 1900, La Plata, Argentina. Consejo Nacional de Investigaciones Científicas y Técnicas (CONICET). vucetich@fcnym.unlp.edu.ar

²Provincia de Buenos Aires; División Paleontología Vertebrados, Museo de La Plata, Paseo del Bosque s/ n, 1900, La Plata, Argentina. Comisión de Investigaciones Científicas (CIC). ceci@fcnym.unlp.edu.ar

³Museo Paleontológico Egidio Feruglio, Av. Fontana 140, U9100GYO Trelew, Argentina. Consejo Nacional de Investigaciones Científicas y Técnicas (CONICET). perezmariae@gmail.com

⁴Facultad de Ciencias Exactas y Naturales, Universidad Nacional de La Pampa, Av. Uruguay 151, 6300 Santa Rosa, Argentina. cmontalvo@exactas.unlpam.edu.ar

Abstract. Living capybaras are a unique group of rodents. They have ever-growing cheek teeth with a complicated occlusal morphology that changes even after birth. Concerning fossil capybaras this morphological change, associated with increasing size, led to regard them as taxonomically highly diverse, including small species with simple dental morphology, and large species with complicated cheek teeth, considered as primitive and derived, respectively. Recently, it was proposed that the different morphs found in each locality actually represent individuals of different ontogenetic stages of a population or successive populations, rather than a multiplicity of coeval species in different stages of evolution. For the Pliocene, the richest locality for capybaras is Farola Monte Hermoso at the southern coast of Buenos Aires Province. This yielded four nominal species of capybaras, three of them are a small morph (*Phugatherium cataclisticum*, “*Anchimyrops villalobosi*”, “*A. ultra*”) and the other a large one (“*Chapalmatherium perturbidum*”). In this paper we propose that they represent juveniles and adults of one species, *P. cataclisticum*. In order to evaluate the phylogenetic position of *Phugatherium* within Caviioidea a cladistic analysis was performed modifying a previously published combined matrix of morphology and DNA sequences. *Phugatherium* forms a monophyletic group and is the sister group of modern capybaras. Within *Phugatherium* the most basal species is *P. novum*, whereas the type species *P. cataclisticum* is the sister group of *P. saavedraei*.

Keywords. Rodentia. Hydrochoeridae. Taxonomy. Pliocene. South America.

Resumen. EL STATUS TAXONÓMICO DE LOS CAPYBARAS (RODENTIA) DEL PLIOCENO *PHUGATHERIUM* AMEGHINO Y *CHAPALMATHERIUM* AMEGHINO. Los carpinchos vivientes son un grupo particular de roedores. Tienen dientes de crecimiento continuo con una complicada morfología oclusal que cambia aún después del nacimiento. En los fósiles, este cambio morfológico asociado al aumento de tamaño llevó a considerarlos muy diversos taxonómicamente, incluyendo especies pequeñas con morfología dentaria simple y especies grandes con molariformes complicados, que fueron consideradas especies primitivas y derivadas, respectivamente. Recientemente se propuso que los diferentes morfos hallados en cada localidad, en realidad representan individuos de diferentes estados ontogenéticos de una o sucesivas poblaciones, más que una multiplicidad de especies contemporáneas en diferentes estados evolutivos. La localidad pliocena más rica en carpinchos es Farola Monte Hermoso, en la costa sur de la Provincia de Buenos Aires. Esta localidad brindó cuatro especies nominales, tres de ellas de un morfo pequeño (*Phugatherium cataclisticum*, “*Anchimyrops villalobosi*”, “*A. ultra*”) y una grande (“*Chapalmatherium perturbidum*”). En este trabajo proponemos que todas ellas representan juveniles y adultos de una especie, *P. cataclisticum*. Para evaluar la posición filogenética de *Phugatherium* entre los Caviioidea, se realizó un análisis cladístico modificando una matriz previa combinada. *Phugatherium* forma un grupo monofilético y es el grupo hermano de los carpinchos vivientes. Dentro de *Phugatherium* la especie más basal es *P. novum*, mientras que la especie tipo, *P. cataclisticum*, es el grupo hermano de *P. saavedraei*.

Palabras clave. Rodentia. Hydrochoeridae. Taxonomía. Plioceno. América del Sur.

LIVING capybaras, *Hydrochoerus hydrochaeris* (Linnaeus, 1766), have many anatomical, biological and behavioral characters that make them a unique group among rodents. They are the largest living rodents and live in herds including males and females of two or three generations. Capybaras have ever-growing cheek teeth with a complicated occlusal morphology

that changes even after birth. Concerning fossil capybaras this morphological change, associated with increasing size, led to regard them from a taxonomical point of view as highly diverse, including small species with relatively simple dental morphology and large species with complicated cheek teeth, originally considered as primitive and derived morphologies,

respectively. Recently, Vucetich *et al.* (2005a, 2012, in press) and Deschamps *et al.* (2007) reanalyzed the late Miocene record of capybaras within a context arisen from the anatomy, ontogeny and social structure of the living species. These authors stated that the different morphs found in each locality, actually represent individuals of different ontogenetic stages of a population or successive populations, rather than a multiplicity of coeval species in different stages of evolution.

For the Pliocene, the richest locality for capybaras is Farola Monte Hermoso at the southern coast of Buenos Aires Province (Fig. 1.1), type locality of the Pliocene Monte Hermoso Formation and Montehermosan Stage/ Age - South American Land mammal Age (SALMA; Deschamps *et al.*, 2012; Tomassini *et al.*, 2013). This is the type locality of four nominal species of capybaras, *Phugatherium cataclisticum* Ameghino, 1887, *Anchimyops villalobosi* Kraglievich, 1927, *A. ultra* Kraglievich, 1941, and *Chapalmatherium perturbidum* (Ameghino, 1888) known as the “gran carpincho corredor” (the large running capybara; Kraglievich, 1941). The first three are known almost exclusively by their holotypes. *P. cataclisticum* is represented only by two mandible fragments and isolated lower cheek teeth, *A. villalobosi* by a palate fragment with upper teeth, and *A. ultra* by an isolated fragment with M2-3. *C. perturbidum* is represented by several skull and mandible fragments even associated ones. *P. cataclisticum*, *A. villalobosi* and *A. ultra* represent a small morphotype bearing

cheek teeth with a simple occlusal morphology, and *C. perturbidum* is a large morphotype with complicated cheek teeth. These species have not been revised since the last paper by Kraglievich (1941; but see a taxonomic revision in Mones, 1973, 1991), although new materials have been discovered. Following the new approach, Vucetich *et al.* (2005a, 2012) and Deschamps *et al.* (2012, 2013) proposed that all the nominal species of the Monte Hermoso Formation actually represent juveniles and adults of a single species, and that by priority its name should be *Phugatherium cataclisticum* Ameghino, 1887. Coincidentally, when revising the materials, we observed that the single specimen of *Anchimyops villalobosi* was identified in schedis also as *P. cataclisticum*, with a peculiar, old handwriting but the author of the label could not be identified yet. In this paper we formalize this proposal and provide evidence supporting the interpretation of the small morphs as juvenile specimens through a revision of the holotypes and new materials from Farola Monte Hermoso. In addition, the holotype of “*Hydrochoerus lydekkeri*” Moreno, 1888, a junior synonym of *C. perturbidum* that was so far lost, was recovered, and is first illustrated together with new materials originally assigned to this species. These taxa are also incorporated to a phylogenetic analysis of extinct and extant cavioids to test the position and monophyly of the genus *Phugatherium*.

Institutional abbreviations. MACN Pv, Museo Argentino

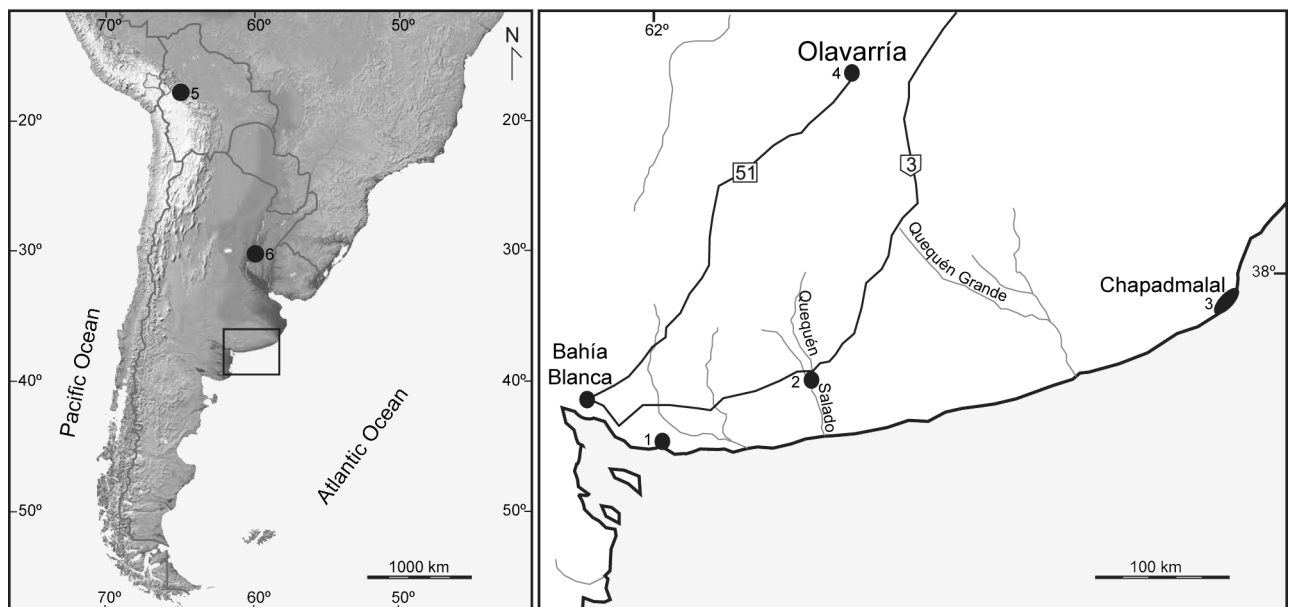


Figure 1. Location map showing localities bearing specimens of *Phugatherium* Ameghino. **1**, Farola Monte Hermoso; **2**, Arroyo Indio Rico (“Irenense”); **3**, Chapadmalal; **4**, Calera Avellaneda, Olavarría; **5**, Ayo Ayo, Bolivia; **6**, Paraná cliffs (“conglomerado osífero”).

de Ciencias Naturales, Vertebrate Paleontology collection, Buenos Aires, Argentina; **MD**, Museo Darwin, Punta Alta, Argentina; **MLP**, Museo de La Plata, La Plata, Argentina; **MMH**, Museo de Monte Hermoso, Monte Hermoso, Argentina; **MMP**, Museo Municipal de Mar del Plata, Mar del Plata, Argentina; **MPEF-PV**, Museo Paleontológico Egidio Feruglio, Paleontología Vertebrados, Trelew, Argentina. **MNHN**, Muséum national d'Histoire naturelle, Paris, France; **FNHM**, Chicago Natural History Museum, Chicago, USA.

Tooth terminology follows Vucetich *et al.*, 2005a and is explained in Fig. 2.

SYSTEMATIC PALEONTOLOGY

Order RODENTIA BOWDICH, 1821

Suborder HYSTRICOGNATHI TULLBERG, 1899

Superfamily CAVIOIDEA (FISCHER DE WALDHEIM, 1817)

KRAGLIEVICH, 1930

Family HYDROCHOERIDAE (GRAY, 1825) GILL, 1872

Genus **Phugatherium** Ameghino, 1887

Type species. *Phugatherium cataclisticum* Ameghino, 1887 (fixed by monotypy).

1887. *Phugatherium* Ameghino.

1908. *Chapalmatherium* Ameghino.

1914. *Protohydrochoerus* Rovereto.

1927. *Anchimysops* Kraglievich partim.

1961. *Neoanchimys* Pascual and Bondesio (see Mones, 1991).

Included species. *Phugatherium cataclisticum*, *Phugatherium* (= *Chapalmatherium*) *novum* (see Deschamps *et al.*, 2012; Chapalmalal Formation, Chapalmalal and El Polvorin For-

mation, Olavarría; Figs. 1.3, 1.4, 3.5), and *Phugatherium* (= *Chapalmatherium*) *saavedrai*, nov. comb. (Umala Formation, Ayo Ayo, Bolivia; Figs. 1.5, 3.6).

Emended diagnosis. Large size; long rostrum and mandibular diastema; P4, M1-2 formed by two independent prisms separated by a very wide H.F.I. and with deep H.P.E. and H.S.E; M3 with 14 to 18 independent prisms in adult specimens, except for the last two to four, which are united in some cases; p4 with very deep h.f.e. and h.s.e.; m1-2 formed by three independent prisms, pr. I V-shaped, pr. IIb Y-shaped.

Distribution. Early Pliocene of South America.

***Phugatherium cataclisticum* Ameghino, 1887**

Figures 2, 3.1–4, 3.7–8, 4, 5

See details of previous list of synonyms in Mones (1991).

1887. *Phugatherium cataclisticum* Ameghino, p. 6.

1888. *Hydrochoerus perturbidus* Ameghino, p. 8.

1888. *Hydrochoerus lydekkeri* Moreno, p. 16.

1914. *Protohydrochoerus perturbidus* Rovereto, p. 141.

1927. *Anchimysops villalobosi* Kraglievich, p. 597.

1934. *Anchimysops* ultra Kraglievich, p. 83 (*nomen nudum*).

1941. *Anchimysops* ultra Kraglievich, p. 322.

1941. *Protohydrochoerus perturbidus lydekkeri* Kraglievich, p. 542.

1958. *Chapalmatherium irenense* Reig, p. 32–40, figs. 1–3.

1961. *Neoanchimys pisanoi* Pascual and Bondesio, p. 101.

1998. *Chapalmatherium perturbidum* Prado *et al.*, p. 791.

Emended diagnosis. Very large size; mandibular diastema long and straight (Figs. 3.8, 5.2, 5.6); P4, M1-2 with very deep H.P.E. and H.S.E., reaching at least 75 % of the transverse diameter of the prism, parallel and perpendicular to de

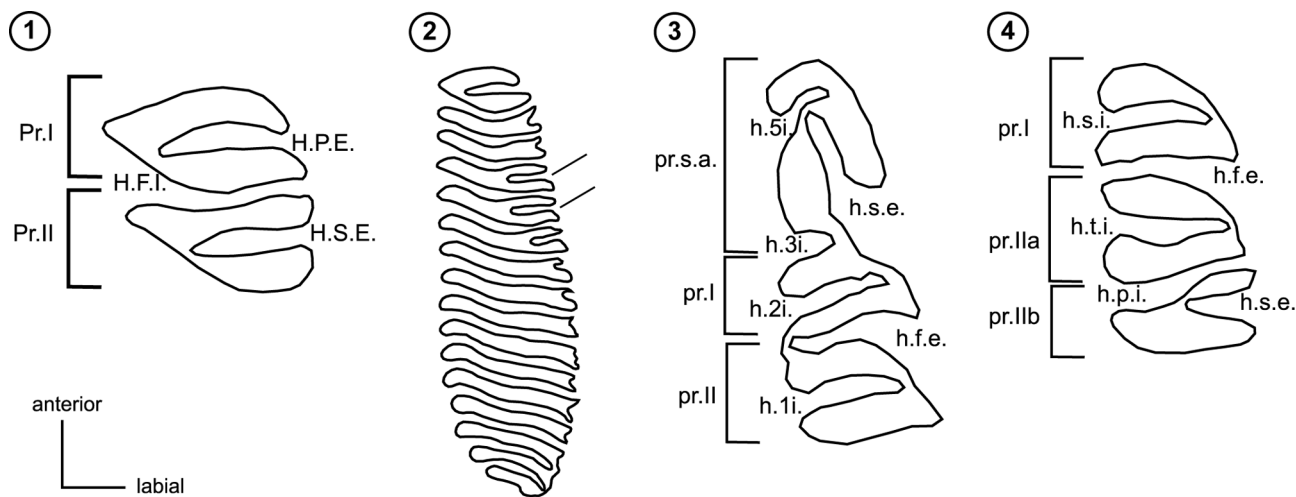


Figure 2. 1-4, *Phugatherium cataclisticum* Ameghino, tooth nomenclature in left upper and lower molars. 1–2, MLP 15-231a, left upper molar; 1, M2 (reversed); 2, M3. 3–4, MACN Pv 7709, left lower molars; 3, p4; 4, m1. Nomenclature follows Vucetich *et al.* (2005a).

AP axis (Figs. 2.1, 5.3); M3 with 16 to 18 independent prisms; Pr.II to Pr.VIII with extraordinary external fissures, those of IV to VI, up to 35 % of the transverse diameter of the prism (Figs. 2.2, 3.8, 5.3); p4 with h.5i. (only absent in MLP 15-232b), h.s.e. very deep, oriented first transversally and then anteriorly to approach the h.5i., h.f.e. deep crossing all the width of the tooth; pr.I and pr.II V-shaped because the h.1i. and h.2i. are very deep (Figs. 2.3, 3.8); pr.I and IIa of m1-2 V-shaped and very deep (Figs. 2.4, 3.7).

The characters of juveniles are as for *Phugatherium cataclisticum* in Mones (1991) (Figs. 3.1–3, 4.1–6). The most anterior prism of p4 (pr.s.a.) is small and lanceolate, only 40 % of the transverse diameter of the tooth; pr.I lanceolate, h.2i.

absent and h.3i. slightly hinted (but in larger specimens these fissures are deeper); pr.II heart-shaped with h.1i. up to 60 % of the transverse diameter of the tooth. The m1 and m2 have lanceolate pr.I with a slight h.s.i., pr.IIa intermediate between lanceolate and laminar with h.t.i. absent, pr.IIb laminar with wide and deep h.s.e. up to 40 % of the transverse diameter of the tooth, in front of the h.p.i., being the latter up to 60 % of the transverse diameter. The pr.I of m3 is not preserved in any specimen, pr.IIa laminar with slight h.t.i. (observed on the lingual wall) and marked but shallow h.t.e., pr.IIb laminar with marked but shallow h.s.e., h.c.i. absent (h.t.e. and h.c.i. sensu Mones, 1991, fig. 6D).

Holotype. MLP 61-VI-7-1a juvenile left fragmentary mandible

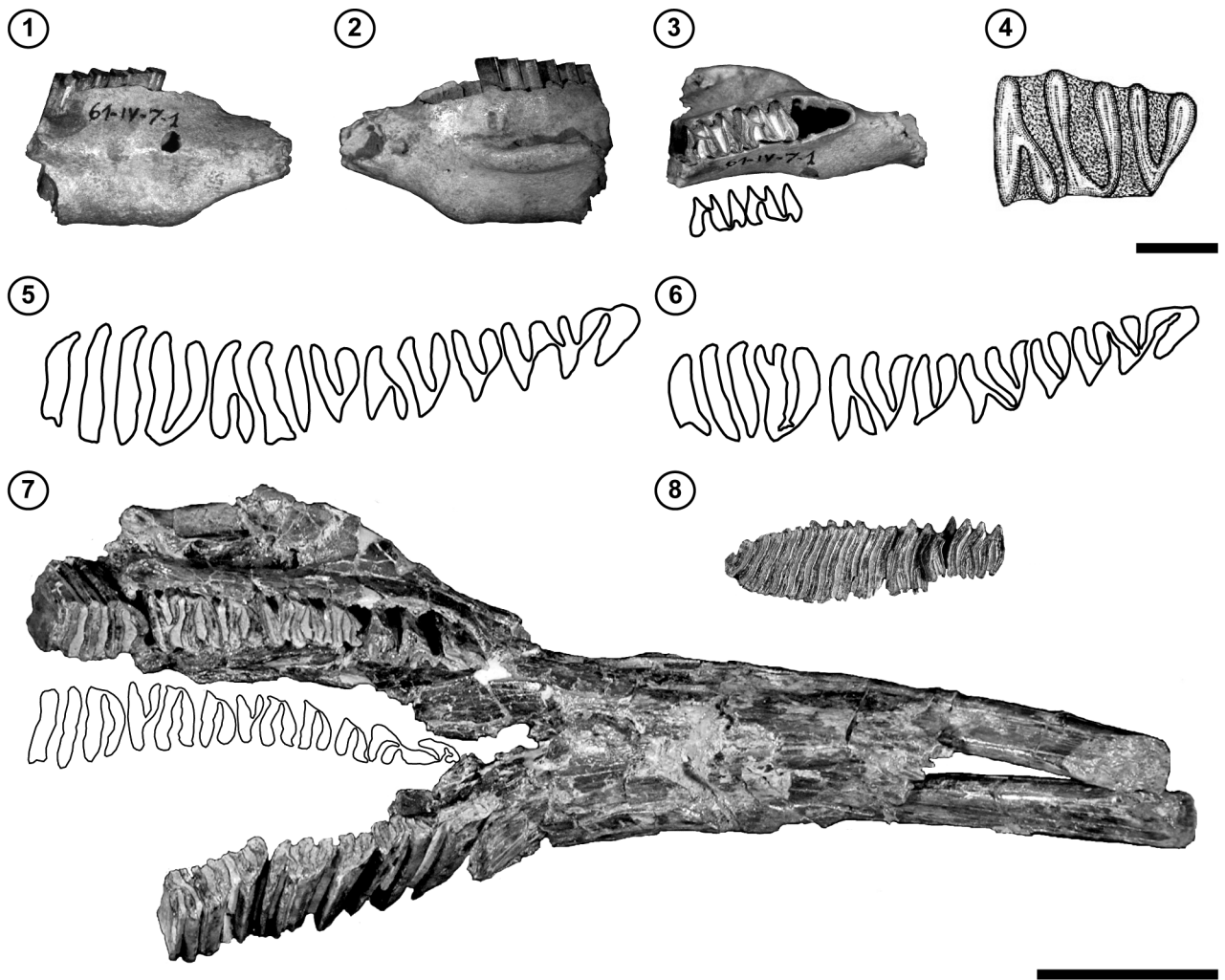


Figure 3. Comparison among mandibles and lower teeth of species of *Phugatherium* Ameghino. 1–3, holotype of *Phugatherium cataclisticum* (MLP 61-IV-7-1) in lingual, labial and occlusal views, with detail of the occlusal surface of m1-2; 4, holotype of *Hydrochoerus perturbidus* (left m1 or m2, specimen lost); 5, *Chapalmatherium novum* (occlusal surface of right p4-m3, MMP 236-5); 6, holotype of *Chapalmatherium saavedrai* (occlusal surface of right p4-m3, MNHN AYO 226); 7–8, holotype of *Hydrochoerus lydekkeri* (MLP 15-232), 7, mandible in occlusal view with detail of the occlusal surface of left p4-m3; 8, left M3 in occlusal view. Scale bar 1–6= 10 mm; 7–8= 50 mm.

with m1-m2 (Figs. 3.1–3).

Holotypes of synonyms. *Protohydrochoerus perturbidus*, right mandibular fragment poorly preserved. This specimen is lost and only a sketch of the m2 (Fig. 3.4) is known (Ameghino, 1889:256); *Anchimysops villalobosi*, MACN Pv 7353, palate with left P4-M3 and right P4-M1 (Fig. 4.1); *Protohydrochoerus rothi*, MACN Pv 7915, left m1-m3 (Fig. 4.2); *Anchimysops ultra*, MACN Pv 9588, left M2 and fragment of M3 (Fig. 4.3); *Hydrochoerus lydekkeri*, MLP 15-232, incomplete mandible with both incisors, left p4-m3 and right p4-m2 (Fig. 3.7), skull fragments with right P4-M2, left M3 (Fig. 3.8) and a fragment of premaxillary with right I; *Neoanchimys pisanoi*, MLP 61-IV-8-1, left p4-m3 (Fig. 4.4); *Chapalmatherium irenense*, FNHM P-14282, right mandibular fragment with p4-m3 (Fig. 4.5) and anterior portion of the skull with damaged left P4-M3 (Fig. 4.6) and right M1-M3.

Referred material. MACN Pv 2480, part of the skeleton (including vertebrae and bones of hind and forelimbs), and left M3; MACN Pv 2928, skull fragment with right M2-M3 and left M3; MACN Pv 7345, isolated juvenile molar and incisor; MACN Pv 7707, mandible fragment with damaged m2-m3; MACN Pv 7709, right mandible with p4-m3 (Fig. 5.1), edentulous palatal fragment and two isolated upper molars; MD 01-03, fragmentary right mandible with p4-m3 (Fig. 5.2); MD-FM 13-01, fragmentary skull with left P4-M3 and right M1-M3 and isolated right and left p4-m3, fragments of upper and lower incisors and fragments of right scapula, humerus, ulna, radius and one carpal; MD-FM 13-02a,b,c, isolated juvenile left m3, left m1 or m2 and right m1 or m2; MD-FM 13-03, juvenile left M3 (Fig. 5.3); MLP 15-231a, fragmentary palate with left P4-M3 and right M3 (Fig. 5.4); MLP 15-231b, fragmentary right mandible with i, p4-m3 and fragment of left i (Fig. 5.5); MLP 48-XII-16-135, isolated left p4 slightly damaged; MLP 57-VII-23-2, left M3; MMH-FM-05-277, right mandible with p4-m3 (Fig. 5.6–8), and MMH-FMH 85-2-18, right and left M1 or M2, left M3, a skull fragment and one vertebra. Other postcranial materials are listed in Mones (1991).

Stratigraphic and geographic provenance. Monte Hermoso Formation, Farola Monte Hermoso, Buenos Aires Province. The holotypes of *Neoanchimys pisanoi*, *Anchimysops ultra*, and *Hydrochoerus lydekkeri*, and MACN Pv 2928, MACN Pv 7707, MACN Pv 7709, MACN Pv 7444, MD-FM 13-03, MLP 15-231a, MLP 15-231b, MMH-FM-05-277, upper

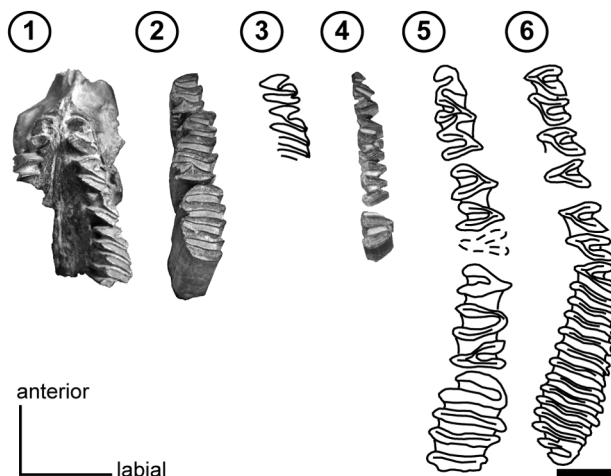


Figure 4. Juvenile specimens of *Phugatherium catacliticum* Ameghino, holotypes of nominal species. **1**, *Anchimysops villalobosi* (palatal fragment, MACN Pv 7353); **2**, *Protohydrochoerus rothi* (left m1-3, MACN Pv 7915); **3**, *Anchimysops ultra* (left M2-M3 in occlusal view, MACN Pv 9588); **4**, *Neoanchimys pisanoi* (left p4-m3 reversed, MLP 61-IV-8-1); **5-6**, *Chapalmatherium irenense* (FNHM P-14282), **5**, right p4-m3, **6**, left P4-M3. Scale bar= 10 mm.

levels; MACN Pv 2840, MD-FM 13-01 and MD-FM 13-02, lower levels. Irene Formation, Quequén Salado River (Fig. 1.2), FNHM P-14282; Paso del Indio Rico, MLP 57-VII-23-2. The remaining materials come from undeterminate levels of the Monte Hermoso Formation, Farola Monte Hermoso.

PHYLOGENETIC AFFINITIES OF PHUGATHERIUM

In order to test the phylogenetic position and monophyly of *Phugatherium* within Caviioidea a cladistic analysis was performed using the combined matrix of morphological and DNA sequences published by Pérez *et al.* (2012). We included three species, *Phugatherium catacliticum*, *P. saavedrai* (Hoffstetter, Villarroel and Rodrigo, 1984), and *Hydrochoeropsis dasseni* Kraglievich, 1930, and redefined some morphological characters, and added new morphological characters. The combined matrix (Supplementary Information 1) for this analysis resulted in 52 taxa, 124 morphological characters (Supplementary Information 2), and 4303 characters from DNA sequences (two nuclear and two mitochondrial genes). The equally weighted parsimony analysis was conducted using TNT 1.1 (Goloboff *et al.*, 2008a, b), performing a heuristic search of 1000 Wagner tree replicates followed by TBR branch swapping, collapsing zero-length branches under the strictest criterion. All morphological characters were

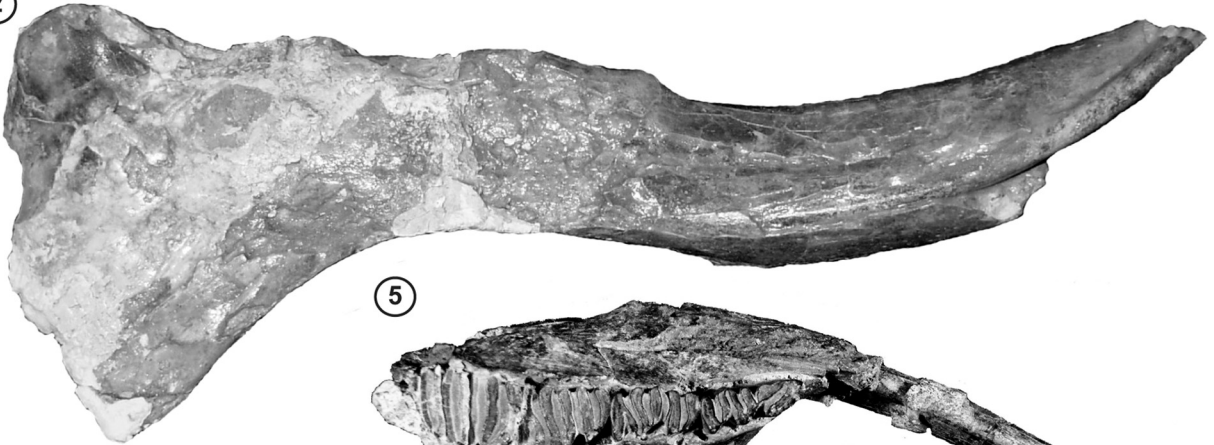
①



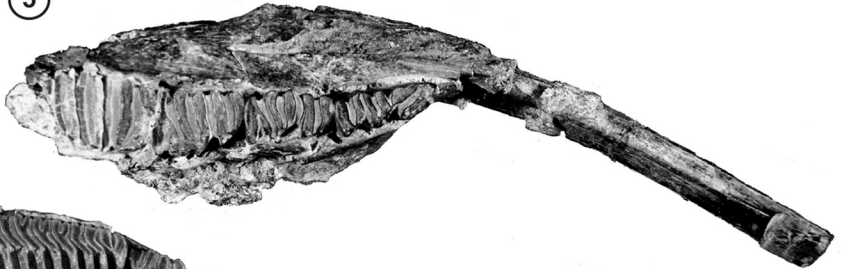
③



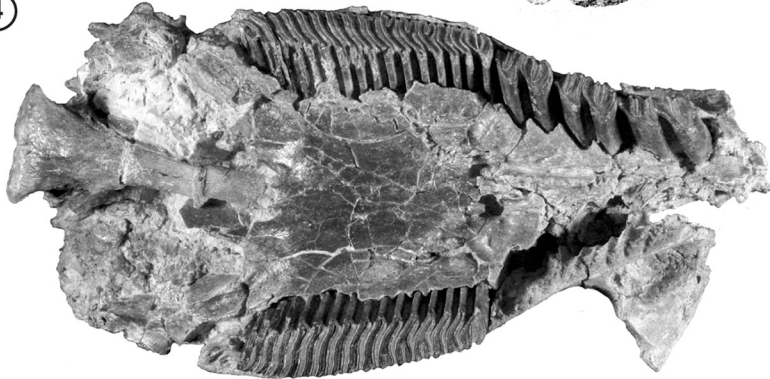
②



⑤



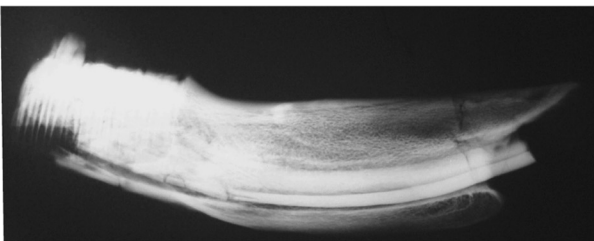
④



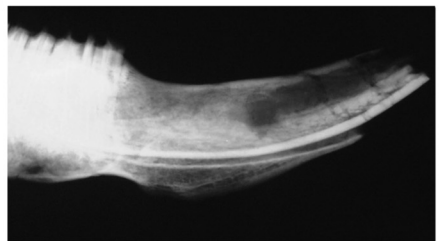
⑥



⑦



⑧



treated as unordered. The transformation cost between transitions and transversions was considered equal and gaps were considered as missing data. In order to test the robustness of the results, support values were calculated using bootstrap and jackknife resampling techniques and Bremer indices in TNT. Unstable taxa in the set of the most parsimonious trees (MPTs) were identified using IterPCR (Pol and Escapa, 2009) to derive an informative reduced consensus.

The combined analysis resulted in a total of 62988 MPTs of 3276 steps (CI= 0.639, RI= 0.513). A strict consensus of all trees was calculated and is shown in the Fig. 6. The crown group shows a basal polytomy due to certain unstable fragmentary fossil taxa (*Allocavia chasicoense* Pascual, *Microcardiodon huemulensis* (Kraglievich), *Cardiomyx andinus* Kraglievich, and *Xenocardia diversidens* Pascual and Bondesio) that take different positions within the crown in the MPTs. When the alternative positions of these species are ignored, the reduced consensus retrieves as monophyletic the lineage that leads to the living capybaras, maras and cavies (Fig. 7).

Phugatherium forms a monophyletic group and is the sister group of *Hydrochoerus*+*Neochoerus* in all MPTs. This clade (node A, Fig. 7) leads to modern capybaras and is supported by three unambiguous synapomorphies: 10 or more lobes in upper third molar (character 37[6]), the transverse extension of the hypoflexus/id (H.F.I. and h.s.e.) crossing completely the tooth (character 53[3]), and the hypoflexus/id (H.F.I. and h.s.e.) of upper and lower first and second molar in occlusal view is canal shaped (character 54[4]).

Within *Phugatherium* (node B, Fig. 7) the most basal species is *P. novum* and the synapomorphies of this genus are: the length of the diastema longer than the molariform series (character 122[1]), the dorsal margin of the lower diastema subparallel (character 123[1]), and the ventral margin of the lower diastema subparallel (character 124[1]).

Within *Phugatherium*, the type species *P. cataclisticum* is the sister group of *P. saavedrai*. The only synapomorphy that supports the close relationships between these two species (node C, Fig. 7) is the depth of h.t.i. in m2 crosses the prism without splitting it (character 43[1]). This condition differs

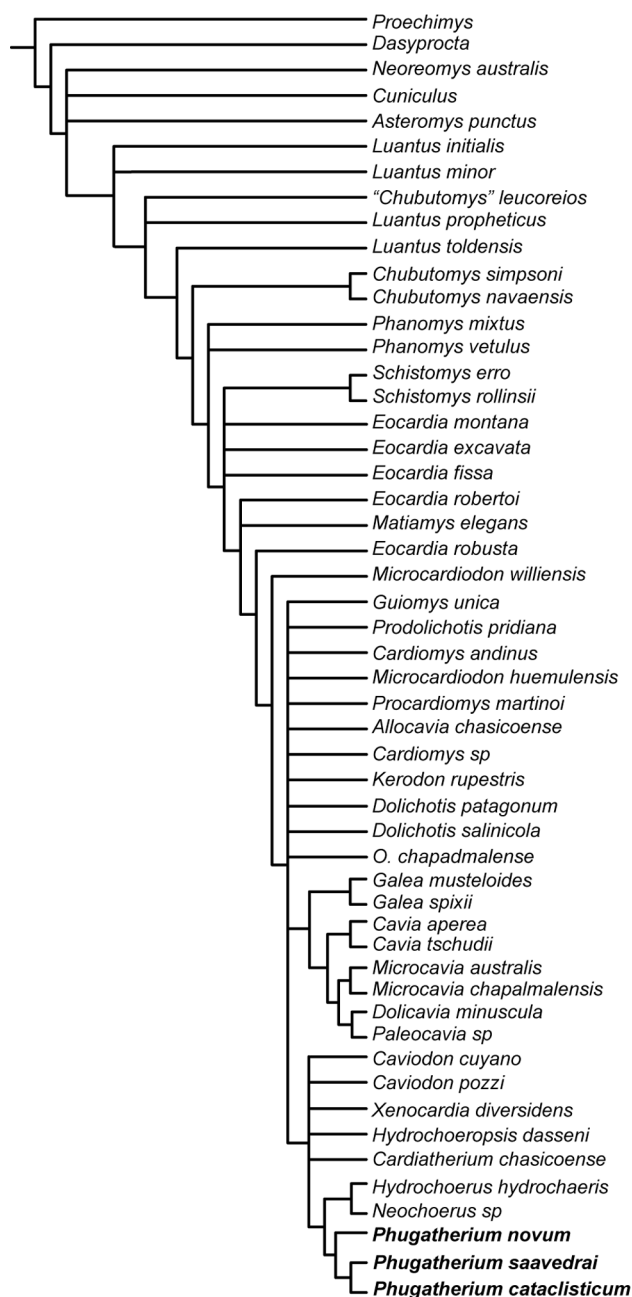


Figure 6. Strict consensus of the 62988 MPTs (length= 3276; CI= 0.639; RI= 0.513) resulting from the parsimony combined analysis of morphological and molecular data set using TNT (see Supplementary Material 1 and 2 of this paper).

from *P. novum* in which the h.t.i. in m2 crosses the prism and splits it, which is the plesiomorphic condition also found in

Figure 5. 1–7, *Phugatherium cataclisticum* Ameghino. 1–2, 4–7, adult specimens; 3, juvenile. 1, MACN Pv 7709, right mandible with p4-m3 in occlusal view; 2, MD-01-03, right mandible in labial view; 3, MD-FM 13-03, left M3; 4-5, MLP 232a and b, a, partial skull with right P4-M3 and left M3, b, right mandible with i, p4-m3; 6–7, MMH-FM-05-277, right mandible with i, p4-m2; 7, X-ray. 8, *Phugatherium novum* Ameghino, MMP-236-S, X-ray of right mandible. Scale bar= 50 mm, except for 3= 10 mm.

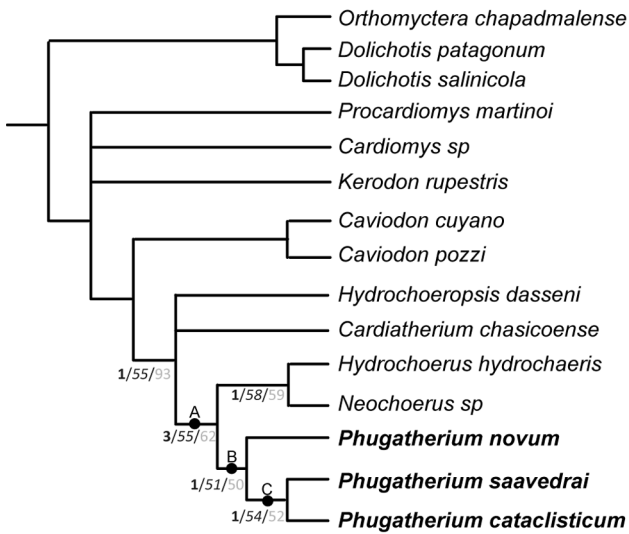


Figure 7. Reduced consensus ignoring the fossil taxa, *Allocavia*, *Microcardiodon huemulensis*, *Cardiomyx andinus* and *Xenocardia*. The numbers in bold indicate Bremer indices, numbers in italics represent absolute jackknife values, and numbers in grey represent absolute bootstrap values.

Neochoerus and some specimens of *Hydrochoerus*.

It is interesting to note that the derived phylogenetic position of *P. cataclisticum* implies that the lineage that leads to the most modern species *P. novum* recorded during the Chapadmalan SALMA would have originated about one million years earlier, during Montehermosan SALMA.

The support values are low for most nodes in the reduced consensus (Fig.7), with Bremer support values of 1 and only a few nodes with frequency values above 50 % in the Jackknife and Bootstrap analyses. The clade formed by *Hydrochoerus*, *Neochoerus*, and *Phugatherium* (node A) shows the highest values (Bremer= 3, Jackknife= 55, Bootstrap= 62) corroborating the close affinities between *Phugatherium* and the modern *Hydrochoerus*.

DISCUSSION

Juvenile characters in *Phugatherium cataclisticum*

The holotypes of *P. cataclisticum* (Figs. 3.1, 3.3) and “*Neoanchimys pisanoi*” (Fig. 4.4), as well as the other lower cheek teeth of the small morphotype, share several characters with juvenile living capybaras, and especially with juveniles of *Cardiatherium paranense* (Ameghino, 1883), from the late Miocene “conglomerado osífero” of the Ituzaingó Formation (Paraná River cliffs, Entre Ríos Province; Fig. 1.6). These juvenile specimens of *C. paranense* were described as *Anchimys*

leidyi, *A. marshi*, and *Procardiatherium simplicidens* (Figs. 6.1–3 respectively) (Vucetich *et al.*, 2005a).

As in the juvenile specimens of *Hydrochoerus hydrochaeris*, molariforms increase in size toward the base of the tooth. The p4, present in the holotype of “*N. pisanoi*” (Fig. 4.4) and MLP 48-XII-16-135, has the most anterior prism (anterior secondary prism, pr.s.a.) conspicuously shorter and more spiky than prism I; this latter is postero-lingually oriented, and the anterior portion of the lingual wall lacks fissures. In MLP 48-XII-16-135, about 20 % larger than the p4 of “*N. pisanoi*”, the lingual wall has two wide but shallow reentrants corresponding to the 2nd and 3rd internal flexiids incipiently developed. A similar morphology is seen in the juveniles “*Anchimys marshi*” and “*Anchimys leidyi*” (Figs. 8.1–2) (Vucetich *et al.*, 2005a). The development of some characters follows also a similar temporal sequence. For example, in the holotype of “*Procardiatherium simplicidens*” (somewhat larger than “*A. marshi*” and “*A. leidyi*”; Fig. 8.3) the 2nd and 3rd flexiids are clearly developed, although shallower than in larger (older) specimens of *Cardiatherium paranense* (Fig. 8.4).

The m1 and m2 of the holotype of “*N. pisanoi*” (Fig. 4.4) have the secondary internal flexid (h.s.i.) very shallow and lack the tertiary internal flexid (h.t.i.), whereas in the holotype of *P. cataclisticum*, somewhat larger than “*N. pisanoi*” the h.s.i. is deeper, and the h.t.i. is already insinuated, especially in m2. In *C. paranense*, this state of relative development, with the h.s.i. deeper than the h.t.i., is only present in MLP 61-VI-8-6, an isolated m1 or m2, intermediate in size between “*Anchimys*” and “*Procardiatherium*”.

The m3 of the holotype of “*N. pisanoi*” (Fig. 4.4) and MD-FM 13-02a has a double secondary external flexid (h.t.e. and h.s.e.; Mones, 1991, fig. 6A,D) as in the holotype of “*A. marshi*” (Fig. 8.4). In the adult (large) specimens of *Cardiatherium* and *Phugatherium* this is a single fissure (Figs. 3.5–6, 8.4).

Two mandibular features also suggest the juvenile character of the small specimens. One is the mandibular symphysis region, which slopes upward in the juveniles of *Hydrochoerus hydrochaeris*, “*Anchimys marshi*”, “*A. leidyi*” (juveniles of *C. paranense*; Fig. 8.1–4) and the holotype of *Phugatherium cataclisticum*, instead of being subhorizontal as in adult specimens (Figs. 5.2, 5.6). The other one is the position of the chin (the posteriormost point of the symphysis) which is ahead the level of the anterior margin of the alveolus of p4 in juveniles

of *Hydrochoerus hydrochaeris*, “*Anchimyds marshi*”, “*A. leidy*”, and the holotype of *P. cataclisticum*, and below this point in adults. In *P. cataclisticum* this shift can be seen even between two adults, one of them smaller (= younger, MMH-FM-05-277) with the chin more anterior than the larger specimen (= older, MD 01-03).

Ontogenetic change

One major issue when interpreting the fossil record of capybaras was that in both localities, the “conglomerado osífero” and the Monte Hermoso Formation at Farola Monte Hermoso, in which there are small capybaras with simple dental structure (without h.t.i.) and large specimens with complex structures, there were no intermediate materials showing the change from one structure to another. Vucetich *et al.*, (2005a) described for the first time this change for the species *Cardiatherium paranense* on the basis of an isolated m1 or m2 (MLP 61-VI-8-6) intermediate in size between the specimens referred to “*Anchimyds*” and those referred to “*Procardiatherium*” and “*Kiyutherium*” (junior synonyms of *Cardiatherium*). These authors interpreted that the beginning of the development of the h.t.i. in *C. paranense* occurred after birth. This transformation should occur relatively quickly because the change in size (age) between the specimen MLP 61-VI-8-6 and the following in size, the holotype of “*Procardiatherium simplicidens*”, is less than 20 % (taking into account the AP of molars). In the living species, the adult molar morphology is accomplished in the first six weeks of life (Mones, 1991). In *Cardiatherium patagonicum* (see Vucetich *et al.*, 2005a) the pattern would be similar to the living species, the unborn specimen MPEF-PV 740/ 21 has already developed the h.s.i. and h.t.i. In *Phugatherium*, the single specimen with lower teeth intermediate in size between the small and large morphotypes is the holotype of *Protohydrochoerus rothi* (MACN Pv 7915) which has already the adult morphology in m1–3. Respect to the palates, the small skull of *Phugatherium novum* MMP 177-S is larger than *Anchimydsops villalobosi* (P4-M2 length 25 mm vs. ca. 16 or 17 mm) and shows the prisms of P4-M3 already separated. Hence, although no materials with an intermediate morphology that allow verifying this change have been found so far, it is here interpreted that the pattern of *Phugatherium cataclisticum* would be more similar to that of *Cardiatherium paranense* with the onset of development of the h.t.i. after birth, than to that of *Cardiatherium patagonicum*

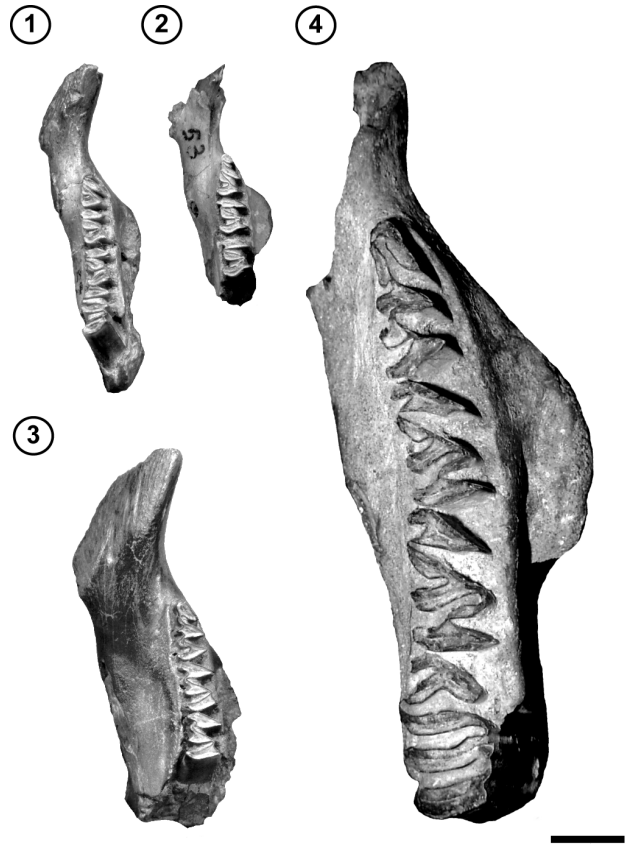


Figure 8. *Cardiatherium paranense* (Ameghino) from the “conglomerado osífero”, Entre Ríos, right mandible. **1–3**, juveniles; **4**, adult. **1**, MLP 73-I-10-7, holotype of *Anchimyds marshi*; **2**, MLP 73-I-10-6, *Anchimyds leidy* (labelled as cotype in MLP); **3**, MLP 73-I-10-8 (reversed), holotype of *Procardiatherium simplicidens*; **4**, MLP 40-XI-15-1, neotype of *Cardiatherium paranensis*. Scale bar = 10 mm.

and the living species in which the onset of the development of the h.t.i. is predisplaced to the intrauterine life.

The morphotype “*Phugatherium*” has been recorded only in Farola Monte Hermoso, favoring its consideration as a small species exclusive of the Monterhermosan. The other localities where the other species of “*Chapalmatherium*” were found have not yielded so far small specimens like the small morphotype “*Phugatherium*”. We think it is simply due to a bias in the record, juveniles are poorly represented in the fossil record.

Individual variation

One of the adult mandibles, MMH-FM-05-277, has a thickening of the bone in the area surrounding the incisor alveolus (Fig. 5.6). This thickening is similar to the one observed in the skull of *Cardiatherium paranense* (MLP 87-XI-1-27) from the “conglomerado osífero” (Vucetich *et al.*, in press) and in the mandible MMP 492-S from the Chapad-

malal Formation (personal observation MGv and CMD). This anomalous bone is likely to be pathological, either by traumatism or disease (Vucetich *et al.*, in press). Through X-ray it could be seen the anomalous bone (Fig. 5.7), compared to a normal one of *Phugatherium novum* (MMP 236-S; Fig. 5.8).

Other variations were observed among the adult specimens of *Phugatherium catacliticum*. In the holotype of *Hydrochoerus lydekkeri* (MLP 15-232; Fig. 3.8) the M3 has a very deep fissure in Pr.II, and the p4 has the Pr.II separated from Pr.I. Concerning the latter feature, this is the largest (oldest) specimen of the sample, and bearing in mind that flexii keep growing through life, at this ontogenetic stage the h.f.e. could have reached the labial wall, cutting it dividing the prism. In this case this could not be considered merely an individual variation, but the result of ontogenetic change in a long-lived individual. In MACN Pv 2840 the Pr.I and Pr.II of M3 are united. In MLP 15-231b the h.5i. is absent in the p4 (Fig. 5.5), and the whole mandible is deformed by the antero-posterior sliding of the area of the teeth over the lower part of the horizontal ramus. In this way, the diastema is shortened and the back of the incisor seems to reach the level of m3 (compare Fig. 3.7 and 5.4). This character of the incisor was described by Kraglievich (1941) who stated that it could be due to post mortem displacement.

Kraglievich (1941) mentioned in the revision of *Protohydrochoerus perturbidus* one character that was present only in the materials found in the upper levels of the exposures of Monte Hermoso. He stated that the lower incisors of these materials which were described as a new species, *Protohydrochoerus* [*Hydrochoerus*] *lydekkeri* by Moreno (1888) had a longitudinal lateral “furrow” (or longitudinal concavity). Although this species had been synonymized by Ameghino (1888), he revalidated the species but with the rank of subspecies, *Protohydrochoerus perturbidus lydekkeri*, for these materials. There is only one specimen from the lower levels of the Monte Hermoso Formation (MD-FM 13-01) preserving the lower incisors. These incisors have no lateral concavity, but the specimen is smaller (younger) than those which have this concavity, and in addition, among the associated post cranial elements, the distal epiphysis of the ulna is not sutured to the diaphysis, suggesting that it is a juvenile. It can be proposed that the longitudinal lateral concavity of lower incisors is acquired with age. More materials from the lower levels are needed in order to test this proposal.

CONCLUSIONS

The revision of Montehermosan capybaras reported here contributes to the study of Mio-Pliocene capybaras accomplished since the paper by Vucetich *et al.* (2005a). According to the phylogenetic analysis, the Pliocene *Phugatherium* is the most closely related to the lineage of modern capybaras, which are recorded since the Pleistocene. *Hydrochoeropsis dasseni* represents another Plio-Pleistocene (“Post-Chapadmalalan”, see Deschamps *et al.*, 2013) lineage not related to the clade *Phugatherium* + (*Nechoerus* + *Hydrochoerus*), showing that at least up to the end of the Pliocene or early Pleistocene, capybaras were quite diverse. As in other caviomorph groups (Hadler *et al.*, 2008; Vucetich *et al.*, 2005b; Vucetich and Verzi, 2002) an important extinction of capybaras occurred during the Pleistocene or even Holocene, being *Hydrochoerus* the single modern representative. The Pleistocene capybaras will be discussed in a forthcoming paper, in order to complete the study of the evolutionary history of these giant rodents.

ACKNOWLEDGEMENTS

The authors thank A.G. Kramarz (MACN) and M.A. Reguero (MLP) for access to materials under their care; T. Manera and the late V. Di Martino for lending us MD-01-03 and FM-05-277 respectively; J. Posik for preparation of MLP 231, MLP 232, MMP 492-S and FM-05-277; W. Acosta for the X-rays. The study was supported by grants UNLP 674, CONICET PIP 0270 (D. Verzi). Comments by A. Mones and an anonymous reviewer certainly improved the manuscript. We thank I. Escapa for his suggestions about figures.

REFERENCES

- Ameghino, F. 1883. Sobre una colección de mamíferos fósiles del piso mesopotamiense de la formación patagónica, recogidos por el Prof. Pedro Scalabrini. *Boletín de la Academia Nacional de Ciencias* (Córdoba) 5: 101–116.
- Ameghino, F. 1887. *Apuntes preliminares sobre algunos mamíferos extinguidos del yacimiento de Monte Hermoso existentes en el “Museo La Plata”*. Imprenta El Censor, Buenos Aires, p. 1–20.
- Ameghino, F. 1888. *Rápidas diagnosis de algunos mamíferos fósiles nuevos de la República Argentina*. P. E. Coni, Buenos Aires, p. 1–17.
- Ameghino, F. 1889. Contribución al conocimiento de los mamíferos fósiles de la República Argentina. *Actas Academia Nacional de Ciencias* 6: 1–1027.
- Ameghino, F. 1908. Las formaciones sedimentarias de la región litoral de Mar del Plata y Chapadmalán. *Anales del Museo Nacional de Buenos Aires* (3) 10: 343–428.
- Bowdich, T.E. 1821. *An analysis of the natural classifications of Mammalia for the use of students and travelers*. Smith, Paris, 115 p.
- Deschamps, C.M., Olivares, A.I., Vieytes, E.C. and Vucetich, M.G. 2007. Ontogeny and diversity of the oldest capybaras (Rodentia, Hydrochoeridae; Late Miocene of Argentina). *Journal of Vertebrate Paleontology* 27: 683–692.
- Deschamps, C.M., Vucetich, M.G., Verzi, D.H. and Olivares, A.I. 2012. Biostratigraphy and correlation of the Monte Hermoso Formation (early Pliocene, Argentina): the evidence from caviomorph rodents. *Journal of South American Earth Sciences* 35: 1–9.
- Deschamps, C.M., Vucetich, M.G., Montalvo, C.I. and Zárate, M.A. 2013. Capybaras (Rodentia, Hydrochoeridae, Hydrochoerinae) and their

- bearing in the calibration of the late Miocene-Pliocene sequences of South America. *Journal of South American Earth Sciences* 48: 145–158.
- Fischer de Waldheim, G. 1817. Adversaria zoologica. Mémoires de la Société Impériale des Naturalistes de Moscou 5: 357–428.
- Gill, T. 1872. Arrangement of the families of mammals with analytical tables. *Smithsonian Miscellaneous Collections* 11: 1–98.
- Goloboff, P., Farris, J. and Nixon, K. 2008a. TNT: Tree analysis using new technology, version 1.1 (Willie Hennig Society Edition). Program and documentation available at <http://www.zmuc.dk/public/phylogeny/tnt>.
- Goloboff, P., Farris, J. and Nixon, K. 2008b. A free program for phylogenetic analysis. *Cladistics* 24: 774–786.
- Gray, J.E. 1825. Outline of an attempt at the disposition of the Mammalia into tribes and families with a list of the genera appertaining to each tribe. *Annals of Philosophy*, New Series 10: 337–344.
- Hadler, P., Verzi, D.H., Vucetich, M.G., Ferigolo, J. and Ribeiro, A.M. 2008. Caviomorphs (Mammalia, Rodentia) from the Holocene of Rio Grande do Sul State, Brazil: systematics and paleoenvironmental context. *Revista Brasileira de Paleontologia* 11: 97–116.
- Hoffstetter, R., Villarroel, C. and Rodrigo, G. 1984. Présence du genre *Chapalmatherium* (Hydrochoeridae, Rodentia) représenté par une espèce nouvelle dans le Pliocène de l'Altiplano bolivien. *Bulletin Museum National d'Histoire Naturelle Paris* 4 (6): 59–79.
- Kraglievich, L. 1927. Nota preliminar sobre nuevos géneros y especies de roedores de la fauna argentina. *Physis* 8: 591–598.
- Kraglievich, L. 1930. La formación friaseana del río Frías, río Fenix, laguna Blanca, etc. y su fauna de mamíferos. *Physis* 10: 127–161.
- Kraglievich, L. 1934. *La antigüedad Pliocena de las faunas de Monte Hermoso y Chapalmalal, deducida de su comparación con las que le precedieron y sucedieron*. Imprenta el Siglo Ilustrado Montevideo, p. 17–136.
- Kraglievich, L. 1941. Monografía del gran carpincho corredor del Plioceno *Protohydrochoerus* (Rovereto) y formas afines. In: A.J. Torcelli and C.A. Morelli (Eds.), *Obras de Geología y Paleontología* 3 (Obras completas y trabajos científicos inéditos), Ministerio de Obras Públicas de la Provincia de Buenos Aires. p. 487–556.
- Linnaeus, C. 1766. *Systema naturae per regna tria naturae, secundum classes, ordines, genera, species, cum characteribus, differentiis, synonymis, locis*. 12^o edition, Stockholm 1: 1–532.
- Mones, A. 1973. Estudios sobre la familia Hydrochoeridae (Rodentia), IV. Elucidación del status de *Phugatherium cataclisticum* Ameghino, 1887. *Ameghiniana* 9: 390–391.
- Mones, A. 1991. Monografía de la Familia Hydrochoeridae (Mammalia, Rodentia). Sistemática–Paleontología–Bibliografía. *Courier Forschungsinstitut Senckenberg* 134: 1–235.
- Moreno, F.P. 1888. Informe preliminar de los progresos del Museo de La Plata durante el primer semestre de 1888. *Boletín del Museo de La Plata* II: 1–35.
- Pascual, R. 1961. Un nuevo Cardiomyinae (Rodentia, Caviidae) de la Formación Arroyo Chasicó (Plioceno inferior) de la provincia de Buenos Aires. *Ameghiniana* 2: 61–72.
- Pascual, R. and Bondesio, P. 1961. Un Nuevo Cardiatheriinae (Rodentia, Hydrochoeridae) de la Formación Monte Hermoso (Plioceno superior) de la provincia de Buenos Aires. Algunas consideraciones sobre la evolución morfológica de los molariformes de los Cardiatheriinae. *Ameghiniana* 2: 93–111.
- Pascual, R. and Bondesio, P. 1963. Un Nuevo tipo de morfología dentaria en un Cardiatheriinae (Rodentia, Hydrochoeridae) del Plioceno inferior de Huachipampa (San Juan). *Ameghiniana* 3: 43–49.
- Pérez, M.E., Vucetich, M.G. and Deschamps, C.M. 2012. Mandibular remains of *Procardiomys martinoi* Pascual, 1961 (Hystricognathi, Caviioidea) from the Arroyo Chasicó Formation (early late Miocene) of Argentina: anatomy and the phylogenetic position of the genus within Caviidae. *Historical Biology*, iFirst article: 1–10. DOI:10.1080/08912963.2012.751383.
- Pol, D. and Escapa, I. 2009. Unstable taxa in cladistic analysis: Identification and the assessment of relevant characters. *Cladistics* 25: 1–13.
- Prado, J.L., Cerdeño, E. and Roig-Juñent, S. 1998. The giant rodent *Chapalmatherium* from the Pliocene of Argentina: new remains and taxonomic remarks on the Family Hydrochoeridae. *Journal of Vertebrate Paleontology* 18: 788–798.
- Reig, O.A. 1958. Sobre una nueva especie del género “*Chapalmatherium*” (Rodentia, Hydrochoeridae), del Plioceno del Río Quequén Salado. *Physis* 21: 32–39.
- Rovereto, C. 1914. Los Estratos Araucanos y sus fósiles. *Anales del Museo Nacional de Historia Natural* 25: 1–147.
- Tomassini, R.L., Montalvo, C.I., Deschamps, C.M. and Manera, T. 2013. Biostratigraphy and biochronology of the Monte Hermoso Formation (early Pliocene) at its type locality, Buenos Aires Province, Argentina. *Journal of South American Earth Sciences* 48: 31–42.
- Tullberg, T. 1899. Über das System der Nagethiere: eine phylogenetische Studie. *Nova Acta Regiae Societatis Scientiarum Upsaliensis* 3: 1–514.
- Vucetich, M.G., Deschamps, C.M., Olivares, A.I. and Dozo, M.T. 2005. Capybaras, shape and time: a model kit. *Acta Palaeontologica Polonica* 50: 259–272.
- Vucetich, M.G., Deschamps, C.M. and Pérez, M.E. 2012. Palaeontology, evolution and systematics of capybaras. In: J.R. Moreira, K.M.P.M. Barros Ferraz, E.A. Herrera, and D.W. Macdonald (Eds.), *Capybara: biology, use and conservation of a valuable Neotropical resource*. Springer, Nueva York, p. 39–59.
- Vucetich, M.G., Deschamps, C.M., Vieytes, E.C. and Montalvo, C.I. (in press). Late Miocene capybaras (Rodentia, Caviioidea, Hydrochoeridae): skull anatomy, taxonomy, evolution and biochronology. *Acta Paleontologica Polonica*. available online 07 Dec 2012 doi: <http://dx.doi.org/10.4202/app.2012.0063>.
- Vucetich, M.G., Vieytes, E.C., Verzi, D., Noriega, J. and Tonni, E.P. 2005. Unexpected primitive rodents in the Quaternary of Argentina. *Journal of South American Earth Sciences* 20: 57–64.
- Vucetich, M.G. and Verzi, D.H. 2002. First record of Dasyproctidae (Rodentia) in the Pleistocene of Argentina. Paleoclimatic implication. *Palaeogeography, Palaeoclimatology, Palaeoecology* 178: 67–73.

SUPPLEMENTARY INFORMATION 2:

Morphological Character List.

Characters with an asterisk (*) are considered “ordered”

1. Mental foramen: absent (0); present (1).
2. Location of the mental foramen on the anterior region of the dentary: close to the dorsal margin of the dentary and opening dorsolaterally (0); at the dorsoventral midpoint of the lateral surface of the dentary and opening laterally (1).
3. Position of the mandibular foramen: behind the retromolar fossa (0); below the m3 (1).
4. Posteroventral projection of the posterior end of the mandibular symphysis: absent (0); present (1).
5. Development of posteroventral projection of the posterior end of the mandibular symphysis in lateral view: well developed, forming an elongate peg exposed in lateral view (0); moderately developed, only a low bulge projects ventrally and is marginally exposed in lateral view (1).
6. Labial edge of the condyle that is the insertion point of *m. masseter posterior*, in posterior view: projecting laterally with respect to wall of the dentary, forming small knob (0); lacking a distinct knob, continuous with lateral wall of the dentary (1).
7. Medial edge of the condyle that is the insertion point of *m. pterygoideus externus*, in posterior view: projecting medially forming a shelf that overhangs the medial surface of the dentary (0); poorly developed projecting medially forming a small knob with respect to medial wall of the dentary (1).
8. Shape of the post-condylar process, in lateral view: squared-off, forming approximately a 90° angle (0); rounded (1).
9. Length of the post-condylar process: equal or longer than the antero-posterior length of the condyle (0); shorter than anteroposterior length

- of the condyle (1).
10. Height of the coronoid process compared to the position of the condyle: located at the same dorsoventral level as the condyle (0); located more ventrally than the condyle (1).
 11. *Anterior margin of the coronoid process: convex (0); straight (1); concave (2).
 12. Dorsal end of the coronoid process: pointed and posterodorsally projected (0); pointed and dorsally projected (1); blunt (2).
 13. *Dorsoventral position of the mandibular notch: located above the occlusal surface of the dental series (0); located at the same height as the occlusal surface of the dental series (1); located ventral to the occlusal surface of the dental series (2).
 14. Shape of the mandibular notch: concave (0); almost straight (1).
 15. *Dorsoventral position of the anterior most point of the lunar notch: low, located ventral to the dorsoventral midpoint of the dentary (between the ventral edge of the dentary and the condyle) (0); located at the approximate dorsoventral midpoint of the dentary (1); high, located above the dorsoventral midpoint of the dentary (2).
 16. Posterior extension of the angular process: level with the post-condylar process (0); ending anterior to the post-condylar process (1); ending posterior to the post-condylar process (2).
 17. *Posterior extension of the root of the lower incisors: extending up to the level of m3 (0); extending up to the level of the posterior lobe of m2 (1); extending up to the level of the anterior lobe of m2 (2); extending up to the level of the posterior lobe of m1 (3); extending up to the level of the anterior lobe of m1 (4).
 18. *Location of the notch for the insertion of the tendon of the *m. masseter medialis pars infraorbitalis* with respect to the toothrow: between p4 and m1 (0); below m1 (1); between m1 and m2 (2).
 19. *Notch for the insertion of the tendon of the *m. masseter medialis pars infraorbitalis*: connected to the masseteric crest (0); isolated, located between the masseteric crest and the horizontal crest (1); connected to the horizontal crest (2).
 20. *Development of the masseteric crest: well developed, forming a shelf that projects laterally with respect to the lateral surface of the dentary (0); forming a well-developed ridge that fails to project with respect to the lateral surface of the dentary (1); absent or poorly developed as a thin and low ridge (2).
 21. Shape of the lateral crest (*sensu* Woods, 1972): straight, projecting anteroventrally from the base of the coronoid process (0); curved, deflecting anteroventrally from the base of the coronoid process (1).
 22. *Anterior origin of the masseteric crest with respect to the toothrow: below m1 (0); below m2 (1); below m3 or posteriorly to m3 (2).
 23. *Posterior extension of the horizontal crest, in lateral view: extending up to the anterior margin of the mandibular condyle (0); approximately ending at the anteroposterior midpoint of the mandibular condyle (1); extending up to the posterior margin of the mandibular condyle (2).
 24. *Development of the horizontal crest: absent or extremely reduced (0); present as a low and broad ridge (1); present as a conspicuous crest, forming a laterally projected shelf but lacking a dorsal fossa (2); well developed, forming a laterally projected shelf and bearing a fossa on its dorsal surface (3).
 25. Depth of the fossa located dorsal to the horizontal crest with respect to the dorsoventral depth of the notch for the insertion of the tendon of the *m. masseter medialis pars infraorbitalis*: notch deeper than fossa (0); fossa deeper than notch (1); notch and fossa equal in depth (2).
 26. Alveolar protuberances (ventral outgrowth of the base of some molari-form alveoli that projects ventrally from the ventral surface of the dentary): absent (0); present (1).
 27. Development of alveolar protuberances: present as a small but distinct convexity on the ventral margin of the dentary (0); present as well-developed bulge on the ventral margin of the dentary (1).
 28. *Degree of hypsodonty: slightly hypsodont, having the root and the anteroposterior length of the occlusal surface longer than the height of the crown (0); mesodont, having the root and the anteroposterior length of the occlusal surface approximately equal to the height of the crown (1); protohypsodont, having the root and the anteroposterior length of the occlusal surface less than half the height of the crown (2); euhypsodont, lacking roots (3).
 29. Developments of lobes in m1-m2: incipient lobes (0); developed lobes (1).
 30. Constriction of the apex in each lobe of the m1-m2: absent (0); present (1).
 31. Shape of the anterior lobe of m1-m2: triangular (0); heart-shaped (1); lanceolate (leaf-shaped) (2); laminar (3).
 32. Shape of the posterior lobe of m1-m2: triangular (0); heart-shaped (1); complex heart-shaped (2).
 33. Shape of the anterior lobe of M1-M2: heart-shaped (0); laminar (1); lanceolate (leaf-shaped) (2).
 34. Shape of the posterior lobe of M1-M2: triangular (0); heart-shaped (1).
 35. Lobes in p4: two incipient lobes (0); two well-developed lobes, but lacking an anterior projection (1); two well-developed lobes and one incipient anterior projection that is not separated from the anterior lobe by an interprismatic furrow (2); two well-developed lobes and one developed anterior projection separated from the anterior lobe by a well-developed interprismatic furrow (3); three lobes (4).
 36. Number of lobes in P4: one (0); two (1).
 37. Number of lobes in M3: one (0); two lobes with an incipient posterior projection (1); two lobes with a developed posterior projection (2); 3-4 with posterior projection (3); 5-6 with posterior projection (4); 7-10 with posterior projection (5); more than 10 lobes.
 38. Longitudinal furrow opposite to hypoflexus/id: absent (0); present (1).
 39. h.s.i. in m1-m2: absent (0); present (1).
 40. Depth of h.s.i. in m1-m2: shallow (0); less than 50 % (1); approximately half of the prisms (50 %) (2); more than 50 % of the prism but not splitting (3).
 41. h.t.i. in m1-m2: absent (0); present (1).
 42. Depth of h.t.i. in m1: up to 50 % of the prism (0); crossing the prism but not splitting (1); crossing and dividing the prism (2).
 43. Depth of h.t.i. in m2: up to 50 % of the prism (0); crossing the prism but not splitting (1); crossing and dividing the prism (2).
 44. Depth of h.s.i. respect to h.t.i. m1: equally deep (0); h.s.i. shallower than h.t.i. (1).
 45. h.p.i. in m1-m2: absent (0); present (1).
 46. Depth of h.s.i. respect to h.p.i. m1: equally deep (0); h.s.i. shallower than h.p.i. (1).
 47. Depth of h.p.i. in m1-m2: shallow (0); up to 25 % (1); up to 50 % (2); reaching the labial end (3); dividing the prism (4).
 48. h.s.e. in m1-m2: absent (0); present (0).
 49. Depth of h.s.e. in m1-m2: shallow, not surpassing the labial end of the h.p.i. (0); up to 50 % of the width of the tooth (1).
 50. H.P.E. in M1-M2: absent (0); present (1).
 51. H.S.E. in M1-M2: absent (0); present (0).
 52. Depth of H.P.E. respect to H.S.E.: equally deep (0); H.P.E. deeper than H.S.E. (1); H.S.E. deeper than H.P.E. (2).
 53. *Transverse extension of the hypoflexus/id: transversely shorter than half of the width of the crown (0); extending from the margin up to the transverse midpoint of the crown (1); extending beyond the transverse midpoint of the crown (2); crossing completely the tooth (3).
 54. Shape of the hypoflexus/id in occlusal view: very narrow and short (0); V-shaped (1); narrow and very long (2); funnel shaped (3); canal shaped (4); V-shaped with blunt end (5).

55. Transverse dentine crest on the occlusal surface, located at the middle of each molar lobe: absent (0); present (1).
56. Length of p4-m1 with respect to the length of the m2-m3 (Wood and Patterson, 1959): p4-m1 shorter than m2-m3 (0); p4-m1 approximately equal to m2-m3 (1).
57. Relative size of lower molars: m1<m2>m3 (0); m1<m2<m3 (1); m1=m2<m3 (2); m1=m2=m3 (3).
58. Relative size of the upper molars: P4<M1<M2 (0); P4>M1<M2 (1); P4>M1=M2 (2); P4>M1>M2 (3).
59. Replacement of deciduous premolar: unreplaced (0); with replacement (1).
60. Type of replacement: postnatal replacement (0); prenatal replacement (1).
61. Orientation of left and right molar series: parallel to each other (0); anteriorly convergent (1).
62. Cement in late ontogenetic stages: absent (0); present (1).
63. Cement in young-adult ontogenetic stages: absent (0); present (1).
64. Cement in juvenile ontogenetic stages: absent (0); present (1).
65. Distribution of enamel in molars: covering the entire crown (0); interrupted at the base of the lingual wall (1); interrupted at the base and the corner of the lingual wall (2); interrupted at the base and in two strips (3); interrupted along the entire labial wall of the upper molars (lingual of the lower molars) except for the flexus/ids opposite to the hypoflexus/id (4); interrupted along the entire lingual wall and antero-lingual and posterolingual walls (5).
66. Fossettes/ids in late ontogenetic stages: present (0); absent (1).
67. Fossettes/ids in young-adult ontogenetic stages: present (0); absent (1).
68. Fossettes/ids in juvenile ontogenetic stages: present (0); absent (1).
69. Shape of the fossettes/ids in m1-m2: elongated (0); subcircular (1).
70. Mesofossettid in young-adult stages: present (0); absent (1).
71. Fusion of the mesolophid with the anterolophid (metalophulid II and metalophulid I respectively *sensu* Marivaux *et al.* 2004): no (0); yes (1). (Kramarz, 2005: character 15).
72. Reduction of the mesolophid (metalophulid II *sensu* Marivaux *et al.* 2004): complete (0), reduced (1). (Kramarz, 2005: character 16).
73. Mesoflexid remains opened: no (0); yes (1). (Kramarz, 2005: character 17).
74. Length of the upper diastema: equal or longer than the molariform series (0); shorter than molariform series (1).
75. Size of oval foramen: small (1); large (0). (Quintana, 1998: character 1).
76. Apex of mesopterygoid fossa with respect to M2: level with M2 (0); apex in front of M2 (1). (Quintana, 1998: character 2).
77. Shape of the apex of mesopterygoid fossa: acuminate (0); curved (1); plane (2).
78. Margens of the mesopterygoid fossa: convergent (0); subparallel (1).
79. Articulation of nasals with respect to premaxillae: nasals articulate with premaxillae throughout their length (0); anterior half of nasals do not articulate with premaxillae (1). (Quintana, 1998: character 6).
80. Shape of frontals: not convex (0); convex (1); markedly convex posteriorly (2). (Quintana, 1998: character 15).
81. Interorbital width: longer or equal to braincase (0); shorter than braincase (1). (Quintana, 1998: character 14).
82. Extension of pterygoids: short (0); long and oriented posteriorly (1). (Quintana, 1998: character 17).
83. Pterygoids: free (0); fused to the auditory bullae (1). (Quintana, 1998: character 18).
84. Length of incisive foramina: long, <50 % (0); short, >50 % (1).
85. Shape of the margins of the incisive foramina: subrectangular (0); fusiform (1); groove like (2); ojival (3); triangular (4).
86. Position of the posterior margin of the upper diastema: not vertical (0); vertical (1). (Quintana, 1998: character 23).
87. Palatal concavity: plane (0); only anterior portion concave (1); concave (2). (Quintana, 1998: character 24).
88. Upper zygomatic process of the maxilla: not extended as plate-shaped in the rostrum (0); plate-shaped (1). (Quintana, 1998: character 25).
89. Shape of upper margin of the infraorbital foramen: not straight (0); with straight upper margin (1). (Quintana, 1998: character 26).
90. Jugular and carotid foramina: fused (0); not fused (1). (Quintana, 1998: character 28).
91. Postfrontal spinous process of the jugal: absent (0); present (1). (Quintana, 1998: character 33).
92. Orbital foramen: fused to the foramen rotundum (0); separated from the foramen rotundum (1). (Quintana, 1998: character 34).
93. Position of upper incisors: orthodont (0); inclined (1). (Quintana, 1998: character 35).
94. Enamel of upper and lower incisors: uncolored (0); with color (1). (Quintana, 1998: character 36).
95. Shape of nasals: not anteriorly vaulted (0); greatly vaulted anteriorly (1). (Quintana, 1998: character 38).
96. Position of parietals: in the same plane with respect to the nasals (0); in different plane with respect to the nasals (1). (Quintana, 1998: character 40).
97. Position of the occipital condyles: below the lower limit of the auditory bullae (0); above the lower limit of the auditory bullae (1). (Quintana, 1998: character 41).
98. Supraorbital foramen or notch: conspicuous (0); absent (1). (Quintana, 1998: character 42).
99. Masseteric fossa of the zygomatic arch: shallow and not well delimited (0); deep and well delimited (1). (Ubilla *et al.*, 1999: character 9).
100. Position of the boundary between the mastoid and paraoccipital processes: at the same level or above the external auditory meatus (0); beneath the external auditory meatus (1). (Ubilla *et al.*, 1999: character 15).
101. Shape of the squamosal process: straight (0); curved (1). (Ubilla *et al.*, 1999: character 18).
102. Shape of the external auditory meatus: long and tube-shaped (0); short (1). (Ubilla *et al.*, 1999: character 19).
103. Posterior apophysis of the squamosal: partially covering the epitympanic sinus (0); completely covering the epitympanic sinus (1).
104. Nasolacrimal foramen in the maxilla: not laterally exposed (0); laterally exposed (1). (Ubilla and Rinderknecht, 2003).
105. Paraoccipital apophyses: short (0); long (1).
106. Jugal: low (0); high (1).
107. Length of ulna bone with respect to length of skull: ulna less or same than skull (0); ulna greater than skull (1). (Quintana, 1998).
108. Length of shin bone with respect to length of skull: shin bone less than skull (0); shinbone greater than skull (1). (Quintana, 1998).
109. Length of radius with respect to length of humerus: radius less than humerus (0); radius greater than humerus (1). (Quintana, 1998).
110. Position of the premaxillary-frontal suture with respect to the tooth series: in front of P4 (0); between p4 and M1 (1); between M1 and M2 (2); from the limit M2-M3 backward (3).
111. Position of the naso-frontal suture with respect to the premaxillary-frontal suture: posterior (0); equal (1); anterior (2).
112. Shape of the ascendant apophysis of the premaxillary: as a thin bar (0); as a wedge, the lateral portion of the premaxillary-maxillary suture goes straight backward (1).
113. Width of the ascendant apophysis of the premaxillary: thin, widened posteriorly (0); thin (1); wide, approximately 50 % the width of the nasal (2).
114. Frontal interposed between nasal and premaxillary: no (0); yes (1).
115. Frontal interposed between premaxillary and maxillary: no (0); yes (1).
116. Lacrimal interposed on the maxillary on the antorbital bar: no (0); yes,

- or leaving a very thin bar of the maxillary.
117. Presence of the lower process of the jugal: present (0); imperceptible (1).
118. Lateral jugal fossa in lateral view: very developed (0); small (1); absent (2).
119. Area between temporal fossae: plane interposed (fossae do not merge on the middle line) (0); sagittal crest (1).
120. Development of the temporal fossae: shallow (0); deep (1).
121. Orientation of the posterior projection of the posterior lobe of M3: antero-posterior (0); transverse (1).
122. Length of the lower diastema: equal or shorter than molariform series (0); longer than the molariform series (1).

123. Dorsal margin of the lower distema: oblique (0); subplane (1).
124. Ventral margin of the lower diastema: oblique (0); subplane (1).

doi: 10.5710/AMEGH.05.02.2014.2074

Recibido: 17 de diciembre de 2013

Aceptado: 05 de febrero de 2014